

Nonlinear vibration analysis of composite laminated trapezoidal plates

Guoqing Jiang¹, Fengming Li^{*1} and Xinwu Li²

¹Beijing Key Laboratory of Nonlinear Vibrations and Strength of Mechanical Structures,
College of Mechanical Engineering, Beijing University of Technology, Beijing 100124, China

²Hong Du Aviation Industry Group, Nan Chang 330024, Jiang Xi, China

(Received July 05, 2015, Revised March 29, 2016, Accepted April 07, 2016)

Abstract. Nonlinear vibration characteristics of composite laminated trapezoidal plates are studied. The geometric nonlinearity of the plate based on the von Karman's large deformation theory is considered, and the finite element method (FEM) is proposed for the present nonlinear modeling. Hamilton's principle is used to establish the equation of motion of every element, and through assembling entire elements of the trapezoidal plate, the equation of motion of the composite laminated trapezoidal plate is established. The nonlinear static property and nonlinear vibration frequency ratios of the composite laminated rectangular plate are analyzed to verify the validity and correctness of the present methodology by comparing with the results published in the open literatures. Moreover, the effects of the ply angle and the length-high ratio on the nonlinear vibration frequency ratios of the composite laminated trapezoidal plates are discussed, and the frequency-response curves are analyzed for the different ply angles and harmonic excitation forces.

Keywords: composite laminated trapezoidal plates; nonlinear vibration; finite element method; frequency ratios; frequency-response curves

1. Introduction

Plates are the main parts of the instruments, mechanical equipments and all kinds of engineering structures. Owing to the unique properties, the composite materials have been extensively used in various engineering fields. The vibration characteristics of composite laminated plates have received considerable attention. In the case of linear vibration, some literatures have studied rectangular plates. Reddy and Kuppusamy (1984) researched the free vibration properties of laminated anisotropic plates. Civalek (2008) applied a four-node discrete singular convolution (DSC) method to analyse the vibration of moderately thick symmetrically laminated composite plates based on the first-order shear deformation theory. Li and Song (2013) investigated the flutter properties of composite laminated panels under the influence of supersonic airflow and thermal effect.

Until now, many researchers have also studied the dynamic properties of irregular plates. Wang *et al.* (2014) developed the differential quadrature method (DQM) to study the vibration of skew

*Corresponding author, Ph.D., Professor, E-mail: fmli@bjut.edu.cn

plate. Zhang *et al.* (2015) analyzed the buckling of FG-CNT reinforced composite thick skew plates using an element-free approach. Taj and Chakrabarti (2013) investigated the static and dynamic properties of functionally graded skew plates under mechanical load using the finite element method (FEM). Ashour (2009) studied the free vibration of fully clamped laminated skew plates employing the finite strip transition matrix method. Civalek (2009) used the DSC method to investigate the free vibration of arbitrary straightsided quadrilateral plates. Karami *et al.* (2003) employed a DQM to analyse the static properties, free vibration and stability of the skewed and trapezoidal composite thin plates.

Gupta and Sharma (2010, 2013) applied the Rayleigh–Ritz method to analyze the thermal effect on the vibration of orthotropic trapezoidal plate and non-homogeneous orthotropic trapezoidal plate. Gürses *et al.* (2009) used the DSC method to research the free vibration characteristics of laminated trapezoidal plates. Zamani *et al.* (2012) investigated the free vibration of moderately thick trapezoidal symmetrically laminated plates with various combinations of boundary conditions. Quintana and Nallim (2013) studied the free vibration of thick trapezoidal and triangular laminated plates resting on elastic supports based on a general Ritz formulation. Catania and Sorrentino (2011) adopted a Rayleigh–Ritz approach to analyze the vibration properties of Kirchhoff plates with general shapes and non-standard boundary conditions.

When the plates are subjected to external loads and the deformations of the plates are large, the nonlinearity problems should be considered, and the nonlinear vibration characteristics of the plates are of great interest to many researchers. Yao and Li (2013) researched the chaotic motion of a composite laminated plate with geometric nonlinearity in subsonic flow based on the von Karman large deflection theory. Amabili (2004) theoretically and experimentally investigated the nonlinear vibrations of rectangular plates with different boundary conditions. Saha *et al.* (2005) analysed the nonlinear free vibration of square plates with various boundary conditions. Tubaldi *et al.* (2014) researched the nonlinear vibrations and stability of a periodically supported rectangular plate in axial flow. Alekar and Rao (1973) studied the nonlinear behaviors of orthotropic skew plates.

Singha and Daripa (2007) and Singha and Ganapathi (2004) studied the nonlinear vibrations of laminated composite skew plates by the FEM. Houmat (2015) analyzed the nonlinear free vibration of variable stiffness symmetric skew laminates. Malekzadeh (2007, 2008) presented large amplitude free vibration analysis of laminated skew plates using a DQM. Shufrin *et al.* (2010) used a semi-analytical approach to analyse the geometrically nonlinear properties of skew and trapezoidal plates subjected to out-of-plane loads. Jaberzadeh *et al.* (2013) applied the element-free Galerkin method to study thermal buckling of functionally graded skew and trapezoidal plates with different boundary conditions.

Although there are some literatures that have studied the vibration properties of irregular plates, most of them are about isotropic skew plates, and very few literatures have studied the composite laminated trapezoidal plates. Moreover, the nonlinearity has been seldom considered and few results on the nonlinear forced vibration properties of the trapezoidal composite laminated plates have been reported. Inspired from these analyses, in the present work, the nonlinear vibration characteristics of composite laminated trapezoidal plates are researched. The von Karman's large deflection theory is considered, and the nonlinear ordinary differential equation of motion of the composite laminated trapezoidal plate is obtained using the FEM. The effects of the ply angle and the length-high ratio on the nonlinear vibration frequency ratios of the composite laminated trapezoidal plates are discussed, and the variations of the frequency-response curves with the different ply angles and harmonic excitation forces are presented.

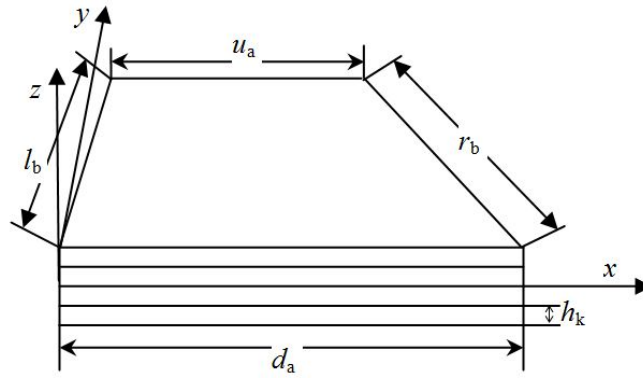


Fig. 1 The composite laminated trapezoidal plates

2. Equation of motion

The composite laminated trapezoidal plate as shown in Fig. 1 is studied. The lengths of the top and bottom edges are u_a and d_a , the lengths of the left and right sides are l_b and r_b , and the thickness of single lamina of the composite laminated plate is h_k . Fig. 1 also shows the Cartesian coordinates of the trapezoidal plate, in which the coordinate origin is located at the left corner and the coordinates x and y are located at the mid-plane of the plate. Three variables u , v and w are used to denote the displacements of the plate in the x , y and z directions.

According to the classical laminated plate theory, the displacement fields of the plate are given as

$$u = u_0 - z \frac{\partial w_0}{\partial x}, \quad v = v_0 - z \frac{\partial w_0}{\partial y}, \quad w = w_0 \quad (1)$$

where u_0 , v_0 and w_0 denote the in-plane and transverse displacements in the x , y and z directions of the mid-plane, and z is the transverse coordinate of the plate.

According to the von Karman's large deformation theory and based on the displacement fields, i.e., Eq. (1), the nonlinear strain-displacement relations are obtained as

$$\{\varepsilon\} = \begin{Bmatrix} \varepsilon_x \\ \varepsilon_y \\ \gamma_{xy} \end{Bmatrix} = \begin{Bmatrix} \frac{\partial u_0}{\partial x} \\ \frac{\partial v_0}{\partial y} \\ \frac{\partial v_0}{\partial x} + \frac{\partial u_0}{\partial y} \end{Bmatrix} + \begin{Bmatrix} \frac{1}{2} \left(\frac{\partial w_0}{\partial x} \right)^2 \\ \frac{1}{2} \left(\frac{\partial w_0}{\partial y} \right)^2 \\ \frac{\partial w_0}{\partial x} \frac{\partial w_0}{\partial y} \end{Bmatrix} + \begin{Bmatrix} -z \frac{\partial^2 w_0}{\partial x^2} \\ -z \frac{\partial^2 w_0}{\partial y^2} \\ -2z \frac{\partial^2 w_0}{\partial x \partial y} \end{Bmatrix} = \{\varepsilon_0\} + \{\varepsilon_l\} + z \{k\} \quad (2)$$

where $\{\varepsilon_0\}$ and $\{\varepsilon_l\}$ represent the membrane strains, and $\{k\}$ represents the bending strain.

According to the orthotropic property of the composite material, the constitutive equation of the k th lamina in the global coordinate system is given by

$$\{\sigma\} = \begin{Bmatrix} \sigma_x \\ \sigma_y \\ \tau_{xy} \end{Bmatrix} = [T][Q][T]^T \begin{Bmatrix} \varepsilon_x \\ \varepsilon_y \\ \gamma_{xy} \end{Bmatrix} = [\bar{Q}]\{\varepsilon\} \quad (3)$$

where $[T]$ is the coordinate transformation matrix, and $[Q]$ is the material elastic constant matrix.

Because the transverse displacement is assumed to be invariable along the thickness of the plate and the triangular plate element is suitable for multiple boundary shapes, the mid-plane of the trapezoidal plate can be discretized by using the triangular plate element. Moreover, the displacements of the element node can be divided into the bending components (w , φ_x , φ_y) and the in-plane components (u , v). So the displacements at arbitrary points of the element can be expressed as follows

$$w_0 = \{H_w\}^T \{w_b\}, \quad u_0 = \{H_u\}^T \{w_u\}, \quad v_0 = \{H_v\}^T \{w_v\} \quad (4)$$

where

$$\begin{aligned} \{w_b\} &= \{w_1 \quad \varphi_{x1} \quad \varphi_{y1} \quad w_2 \quad \varphi_{x2} \quad \varphi_{y2} \quad w_3 \quad \varphi_{x3} \quad \varphi_{y3}\}^T \\ \{w_u\} &= \{u_1 \quad u_2 \quad u_3\}^T, \quad \{w_v\} = \{v_1 \quad v_2 \quad v_3\}^T, \\ \{H_w\} &= \{N_1 \quad N_{x1} \quad N_{y1} \quad N_2 \quad N_{x2} \quad N_{y2} \quad N_3 \quad N_{x3} \quad N_{y3}\}^T \\ \{H_u\} &= \{L_1 \quad L_2 \quad L_3\}^T, \quad \{H_v\} = \{L_1 \quad L_2 \quad L_3\}^T, \\ N_i &= L_i + L_i^2 L_j + L_i^2 L_m - L_i L_j^2 - L_i L_m^2 \\ N_{xi} &= b_j L_i^2 L_m - b_m L_i^2 L_j + (b_j - b_m) L_i L_j L_m / 2 \\ N_{yi} &= c_j L_i^2 L_m - c_m L_i^2 L_j + (c_j - c_m) L_i L_j L_m / 2, \\ a_i &= x_j y_m - x_m y_j, b_i = y_j - y_m, c_i = x_m - x_j, \\ i &= 1-2-3, j=2-3-1, m=3-1-2, \end{aligned}$$

in which L_1, L_2, L_3 , are the area coordinates of the triangular plate element, and φ_x and φ_y are the derivatives of the lateral deflection, i.e., $\varphi_{xi} = (\partial w / \partial y)_i$ and $\varphi_{yi} = (\partial w / \partial x)_i$.

Because Eq. (4) is expressed in the area coordinates (it may also be called the natural coordinates system) and other formulas established are in the physical coordinates system, those formulas established should be transformed into the natural coordinates system. The conversion relationships are expressed as

$$\begin{Bmatrix} L_1 \\ L_2 \\ L_3 \end{Bmatrix} = \frac{1}{2A} \begin{bmatrix} a_1 & b_1 & c_1 \\ a_2 & b_2 & c_2 \\ a_3 & b_3 & c_3 \end{bmatrix} \begin{Bmatrix} 1 \\ x \\ y \end{Bmatrix}, \quad dxdy = |J| dL_1 dL_2 = 2A dL_1 dL_2, \quad (5)$$

where J is the Jacobi matrix, and A is the surface area of the plate.

Hamilton's principle is used to formulate the governing equation of motion, and it is expressed as

$$\int_{t_1}^{t_2} \delta(T - U) dt + \int_{t_1}^{t_2} \delta W dt = 0, \quad (6)$$

where T , U and δW are the kinetic energy, the strain energy and the virtual work done by the external loads, and they are obtained as

$$T = \frac{1}{2} \int_V \rho (\dot{u}^2 + \dot{v}^2 + \dot{w}^2) dV, \quad U = \frac{1}{2} \int_V \{\varepsilon\}^T \{\sigma\} dV, \quad (7a)$$

$$\delta W = \int_A \{\delta w_b\}^T \{H_w\} p dA + \sum_{i=1}^N \{\delta w_b\}^T \{H_w\}_{(x_i, y_i)} F_i, \quad (7b)$$

where V is the volume of the plate, ρ is the mass density of the material, p is the distributed load in the z direction, and F_i is the concentrated force which is located at position (x_i, y_i) .

T , U and δW are calculated by substituting Eqs. (1)-(4) into Eq. (7), and then they are substituted into Eq. (6). By performing the variation operation, the equation of motion of the element is obtained, and by assembling the element mass and stiffness matrices into the global ones, the equation of motion of the composite laminated trapezoidal plates can be obtained as follows

$$[M]\{\ddot{w}\} + [C]\{\dot{w}\} + ([K_l] + [K_{nl}])\{w\} = \{F\}, \quad (8)$$

where $\{w\} = [u_1, v_1, w_1, \varphi_{x1}, \varphi_{y1}, \dots, u_n, v_n, w_n, \varphi_{xn}, \varphi_{yn}]^T$ is the nodal displacement vector in which n is the number of the node of the trapezoidal plate, $[M]$ is the mass matrix, $[C]$ is the damping matrix, $[K_l]$ and $[K_{nl}]$ are the linear and nonlinear stiffness matrices, and $\{F\}$ is the excitation force vector. The elements of the mass and stiffness matrices are listed in the Appendix.

3. Numerical simulations and discussions

3.1 Validations of the formulations and codes

The numerical simulations are performed by the MATLAB software. In order to verify the correctness of the governing equation of motion and the MATLAB programs, the static responses of the anisotropic plates obtained by the present method are compared with those of Reddy (2004) as shown in Table 1. The geometrical sizes and material properties of the composite laminated rectangular plate used in the calculation are: the length and width are $a = b = 12$ in, the thickness is $h = 0.138$ in, $E_1 = 3 \times 10^6$ psi, $E_2 = 1.28 \times 10^6$ psi, $\mu_{12} = 0.32$, $\mu_{21} = 0.1365$, $G_{12} = 0.37 \times 10^6$ psi. The boundary conditions considered here are:

- (a) Simply supported condition: $u_0 = v_0 = w_0 = 0$, at $x = 0, a$ and $y = 0, b$.
- (b) All edges clamped condition: $u_0 = v_0 = w_0 = \varphi_x = \varphi_y = 0$

Furthermore, the variations of the nonlinear frequency ratio ω_{NL}/ω_L with respect to the maximum amplitude of the plate w_{\max} are computed for simply supported square plates, in which

Table 1 The static responses of all edges clamped anisotropic rectangular plates under uniform load

	q_0/psi	0.5	1.0	4.0	8.0	12.0	16.0	20.0
Reddy (2004)	w_0/in	0.0294	0.0552	0.1456	0.2054	0.2450	0.2754	0.3006
Present results	w_0/in	0.0326	0.0592	0.1424	0.1958	0.2313	0.2587	0.2816

Table 2 Comparison of nonlinear frequency ratios (ω_{NL}/ω_L) of simply supported anisotropic plates

w/h	0.2	0.4	0.6	0.8	1.0
Bhimaraddi (1993)	1.0196	1.0761	1.1642	1.2774	1.4097
Mei and Decha-Umphai (1985)	1.0134	1.0518	1.1154	1.1946	1.2967
Singha and Daripa (2007)	1.0190	1.0739	1.1597	1.2699	1.3987
Present results	1.0137	1.054	1.1182	1.2034	1.3063

the subscripts NL and L represent the nonlinear and linear cases. The present results are compared with those in the open literatures as shown in Table 2. The material properties and geometrical sizes of the composite square plate used in the calculation are: $E_1 = 4 \times 10^6$, $E_2 = 1 \times 10^5$, $\rho = 1$, $G_{12} = 0.5 \times 10^5$, $\mu_{12} = 0.25$, $\mu_{21} = 0.00625$, the length and width are $a = b = 1000 \times h$, and the thickness is $h = 0.003$.

It is observed from Tables 1 and 2 that the present results match quite well with those in the open literatures, which verifies that the governing equation of motion obtained in this paper and the MATLAB programs are correct.

3.2 Nonlinear vibration analysis

In this section, the nonlinear vibration properties of the composite laminated trapezoidal plates are investigated. The material properties used in the calculation are: $E_1 = 40 \times 10^9$ Pa, $E_2 = 1 \times 10^9$ Pa, $\rho = 1000 \text{ kg/m}^3$, $G_{12} = 0.5 \times 10^9$ Pa, $\mu_{12} = 0.25$, $\mu_{21} = 0.00625$. The geometrical sizes are $d_a = 0.3$ m, $u_a = 0.135$ m, $l_b = 0.21$ m, $r_b = 0.26$ m, and the single lamina thickness is $h = 0.003$ m. The height of the trapezoidal plate is denoted by L . The boundary conditions are as follows:

$$u_0 = v_0 = w_0 = \varphi_x = \varphi_y = 0, \text{ at } y = 0, L.$$

$$u_0 \neq 0, v_0 \neq 0, w_0 \neq 0, \varphi_x \neq 0, \varphi_y \neq 0, \text{ at } l_b \text{ and } r_b \text{ edges.}$$

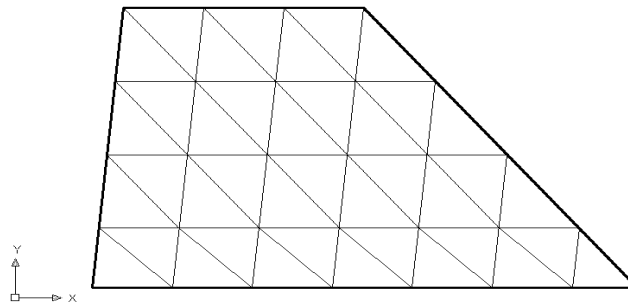


Fig. 2 The mid-plane of the composite laminated trapezoidal plates

Table 3 The convergence of linear natural frequencies of the composite trapezoidal plate

Element number	21	40	65
Linear frequency			
ω_1	1447.4	1474.6	1493.7
ω_2	2754.7	2091.1	2125.4

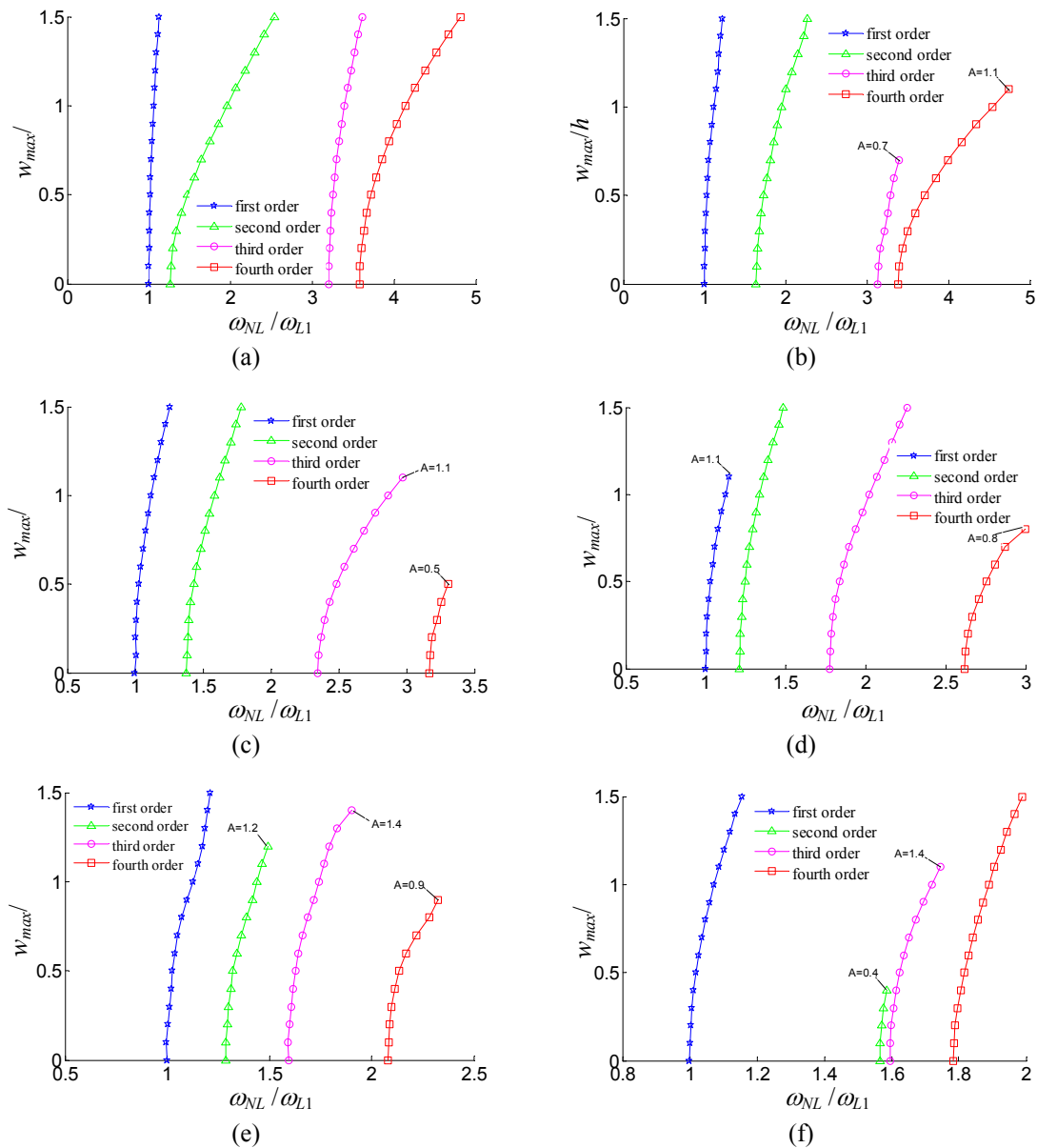


Fig. 3 The relationship curves of nonlinear frequency ratios and amplitudes at certain ply angles for different modes of the trapezoidal plate: (a) $[0^\circ/0^\circ]$; (b) $[30^\circ/-30^\circ]$; (c) $[45^\circ/-45^\circ]$; (d) $[60^\circ/-60^\circ]$; (e) $[75^\circ/-75^\circ]$; (f) $[90^\circ/-90^\circ]$

First of all, the mid-plane of the trapezoidal plate is discretized to triangular plate elements as shown in Fig. 2. It is advantageous to divide the meshes in this way for the theoretical analysis. The convergence of the first two linear natural frequencies for all edges clamped composite trapezoidal plate is presented in Table 3. Furthermore, the nonlinear free vibration properties of the composite laminated trapezoidal plates are analysed. Fig. 3 shows the relationship curves of nonlinear vibration frequency ratios and maximum amplitudes at different ply angles for different modes. In the figures, the point A represents that the nonlinear frequency cannot be obtained at this maximum amplitude, because the vibration of the plate may be affected by the strong nonlinearity and this can lead to the vibration being uncertainty. ω_{L1} is the linear natural frequency with each ply angle.

It can be seen from the figures that the effects of nonlinearity at each ply angle for the different modes can be observed by the gradients of the curves. The nonlinear frequencies between the first and fourth, and the second and third are closer with the ply angle increasing.

It can also be known from Fig. 3 that with the amplitude increasing, the nonlinear frequency ratio increases gradually. For every nonlinear frequency, the effect of nonlinearity on the frequency depends on the ply angle. It can be seen that the effect of the nonlinearity on the first and fourth nonlinear frequencies increases with the ply angle increasing from 0° to 60° , and then it decreases with the ply angle increasing from 60° to 90° . The effect of the nonlinearity on the second nonlinear frequency increases with the ply angle increasing. For the third nonlinear frequency, the effect of the nonlinearity increases with the ply angle increasing from 0° to 30° , decreases with ply angle increasing from 30° to 60° , and then increases with the ply angle increasing from 60° to 90° .

Table 4 shows the variations of the nonlinear vibration frequency ratios (ω_{NL1}/ω_{L1}) with respect to the maximum amplitudes under the different ply angles. Here, ω_{NL1}/ω_{L1} represents the ratio of the first nonlinear frequency and the first linear natural frequency.

The contours of amplitude distribution of the trapezoidal plate at $w_{\max}/h = 1.5$ is shown in Fig. 4. It can be seen that the amplitude distribution shapes are associated with the ply angle. The region corresponding to the maximum amplitude becomes narrow with the ply angle increasing, and the regional size where the counter appears moves to the right side of the plate with the increase of ply the angle. Especially, it can be noted that, for the ply angle $[90^\circ/-90^\circ]$, in a larger area of the trapezoidal plate the contour cannot be observed. This is because the amplitude is so small that it is negligible.

Next, the effect of the length-height ratio (d_a/L) on the nonlinear frequency ratio is studied. The nonlinear frequency ratios (ω_{NL1}/ω_{L1}) of two layer composite laminated trapezoidal plates with

Table 4 The nonlinear frequency ratios (ω_{NL1}/ω_{L1}) of two layer composite laminated trapezoidal plates

w/h	0.1	0.3	0.5	0.7	0.9	1.0	1.2
Cross-ply							
$[0^\circ/0^\circ]$	1.00057	1.00517	1.01442	1.02827	1.04651	1.05717	1.08138
$[15^\circ/-15^\circ]$	1.00036	1.00568	1.02144	1.03437	1.06548	1.07079	1.10152
$[30^\circ/-30^\circ]$	1.00025	1.01256	1.02313	1.04727	1.09493	1.1153	1.16076
$[45^\circ/-45^\circ]$	1.00202	1.00868	1.02673	1.05439	1.10209	1.12821	1.16258
$[60^\circ/-60^\circ]$	1.00101	1.01063	1.03006	1.05887	1.09686	1.12519	--
$[80^\circ/-80^\circ]$	1.00021	1.00667	1.02932	1.05448	1.0865	1.10483	1.12382
$[90^\circ/-90^\circ]$	1.00077	1.00693	1.01907	1.03684	1.0598	1.07306	1.10279

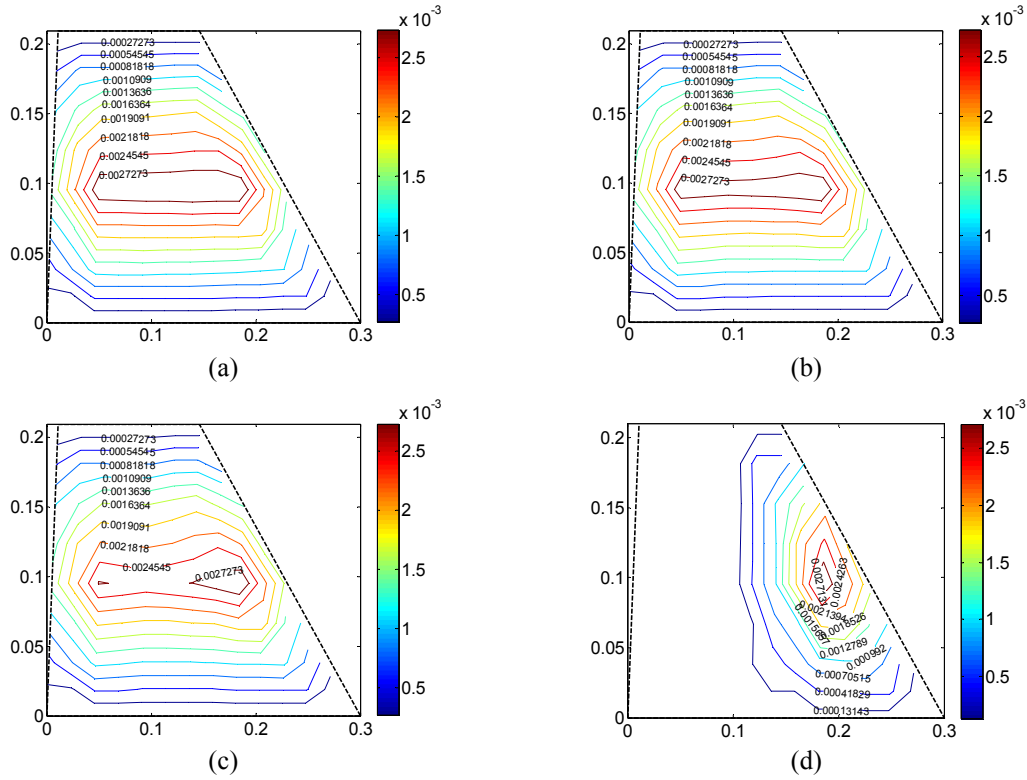


Fig. 4 The contours of amplitude distribution of the trapezoidal plate at $w_{\max}/h = 1.5$ under the different ply angles, (a) $[0^\circ/0^\circ]$; (b) $[30^\circ/-30^\circ]$; (c) $[45^\circ/-45^\circ]$; and (d) $[90^\circ/-90^\circ]$

Table 5 The nonlinear frequency ratios (ω_{NL1}/ω_{L1}) of two layer composite laminated trapezoidal plates with different length-height ratios (d_a/L)

Ply angle	Cross-ply	w/h						
		0.1	0.3	0.5	0.7	0.9	1.0	1.2
$[0^\circ/0^\circ]$	1.7141	1.00061	1.00552	1.01523	1.02955	1.04819	1.05902	1.08349
	1.4306	1.00057	1.00517	1.01442	1.02827	1.04651	1.05717	1.08138
	1.2856	1.00077	1.00693	1.01921	1.03738	1.06107	1.07486	1.106
$[45^\circ/-45^\circ]$	1.7141	1.00113	1.01389	1.03723	1.06576	--	--	--
	1.4306	1.00202	1.00868	1.02673	1.05439	1.0209	1.12821	1.16258
	1.2856	1.00251	1.01313	1.04633	1.07626	1.13863	1.15282	1.23272
$[45^\circ/-45^\circ]$	1.7141	1.00075	1.00671	1.01843	1.03558	1.05771	1.07049	1.09916
	1.4306	1.00077	1.00693	1.01907	1.03684	1.0598	1.07306	1.10279
	1.2856	1.00133	1.01182	1.03196	1.06036	1.09542	1.11498	1.15732

different length-height ratios are shown in Table 5. It can be observed that for any ply angle and for any certain amplitude, with the length-height ratio decreasing, the nonlinear frequency ratio becomes generally large, which means that with the length-height ratio decreasing, the effect of

nonlinearity of the plate is severe. For the given length-height ratios, the nonlinear frequency ratio with respect to the maximum amplitude is larger when the ply angle is $[45^\circ/-45^\circ]$.

The nonlinear forced vibration properties of the composite laminated trapezoidal plates are also studied. In order to research the resonant properties of the plate, the positions of the harmonic excitation force and the observation point of frequency-response curve at the trapezoidal plate are all at $x = 0.09513$, $y = 0.09532$. Assume that the structural damping is $c = 0.00125$. Fig. 5 shows

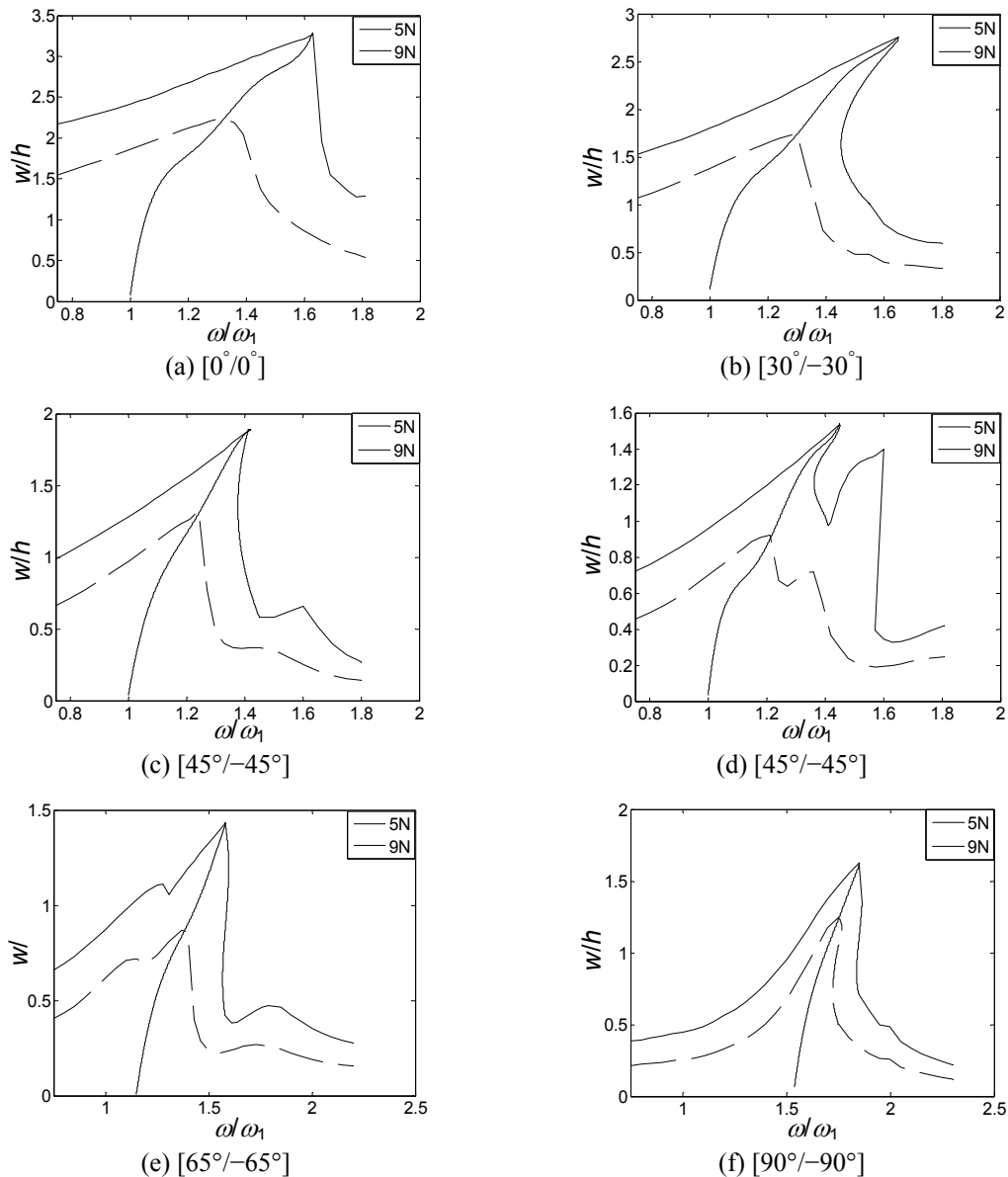


Fig. 5 The frequency-response curves of trapezoidal plates under different ply angles and different external forces, (a) $[0^\circ/0^\circ]$; (b) $[30^\circ/-30^\circ]$; (c) $[45^\circ/-45^\circ]$; (d) $[60^\circ/-60^\circ]$; (e) $[65^\circ/-65^\circ]$; and (f) $[90^\circ/-90^\circ]$

the frequency-response curves of the trapezoidal plates under different ply angles and different external forces. Here, the backbone curves are obtained through linking the peak values of the responses for the different excitation forces. The figure shows that the nonlinear resonance properties are dependent on the backbone curves.

Especially, it can be observed from Figs. 5(c)-(f) that the second nonlinear resonance of the composite laminated trapezoidal plate also appears. This is because that for the given ply angles the first and the second linear natural frequencies are near. With the ply angle increasing, the amplitude of the first nonlinear resonance becomes smaller, and the amplitude of the second nonlinear resonance becomes larger. Moreover, it is interesting that only the second nonlinear resonance can be seen from Fig. 5(f), and the backbone curve in the figure starts from $\omega/\omega_1 = 1.54$ which is equal to ω_2/ω_1 . Fig. 5 also shows that the amplitude of resonance and the first nonlinear resonance frequency all decrease with the ply angle increasing, which means that the effect of the nonlinearity is weakened.

4. Conclusions

The nonlinear vibration characteristics of the composite laminated trapezoidal plates are studied. The equation of motion of the composite laminated trapezoidal plate is established by the FEM and Hamilton's principle. The effects of the ply angle and length-height ratio on the nonlinear vibration frequency ratio of the composite laminated trapezoidal plates are discussed, and the frequency-response curves are analyzed for the different ply angles and harmonic excitation forces. From the numerical simulation, the following conclusions can be drawn:

- (1) The nonlinear frequency ratio increases gradually with the maximum amplitude increasing, and the effect of nonlinearity on the nonlinear vibration frequency ratio depends on the ply angle.
- (2) With the ply angle increasing, the region corresponding to the maximum amplitude of the trapezoidal plate is decreased, and the regional size where the counter appears moves to the long side (right side) of the composite laminated trapezoidal plate.
- (3) For any ply angle and any certain maximum amplitude, the effect of nonlinearity on the plate is severe with the length-height ratio decreasing. For the given length-height ratios, the nonlinear frequency ratios with respect to the maximum amplitudes are larger when the ply angle is $[45^\circ/-45^\circ]$.
- (4) The nonlinear resonance is dependent on the backbone curve. With the ply angle increasing, the amplitude and the first nonlinear resonance frequency decrease, which means that the effect of the nonlinearity is weakened. The second nonlinear resonance of the trapezoidal composite laminated plate also appears with the ply angle increasing. Especially, it is interesting that when the ply angle is increased to $[90^\circ/-90^\circ]$, only the second nonlinear resonance can be seen.

Acknowledgments

This research is supported by the National Natural Science Foundation of China (No. 11172084, 11572007).

References

- Alear, R.S. and Rao, N.S. (1973), "Nonlinear analysis of orthotropic skew plates", *AIAA Journal*, **11**(4), 495-498.
- Amabili, M. (2004), "Nonlinear vibrations of rectangular plates with different boundary conditions: theory and experiments", *Comput. Struct.*, **82**(31-32), 2587-2605.
- Ashour, A.S. (2009), "The free vibration of symmetrically angle-ply laminated fully clamped skew plates", *J. Sound Vib.*, **323**(1-2), 444-450.
- Bhimaraddi, A. (1993), "Large amplitude vibrations of imperfect antisymmetric angle-ply laminated plates", *J. Sound Vib.*, **162**(3), 457-470.
- Catania, G. and Sorrentino, S. (2011), "Spectral modeling of vibrating plates with general shape and general boundary conditions", *J. Vib. Control*, **18**(11), 1607-1623.
- Civalek, O. (2008), "Free vibration analysis of symmetrically laminated composite plates with first-order shear deformation theory (FSDT) by discrete singular convolution method", *Finite Elem. Anal. Des.*, **44**(12-13), 725-731.
- Civalek, O. (2009), "A four-node discrete singular convolution for geometric transformation and its application to numerical solution of vibration problem of arbitrary straight-sided quadrilateral plates", *Appl. Math. Model.*, **33**(1), 300-314.
- Gupta, A.K. and Sharma, S. (2010), "Thermally induced vibration of orthotropic trapezoidal plate of linearly varying thickness", *J. Vib. Control*, **17**(10), 1591-1598.
- Gupta, A.K. and Sharma, S. (2013), "Effect of thermal gradient on vibration of non-homogeneous orthotropic trapezoidal plate of linearly varying thickness", *Ain Shams Eng. J.*, **4**(3), 523-530.
- Gürses, M., Civalek, Ö., Ersoy, H. and Kiracioglu, O. (2009), "Analysis of shear deformable laminated composite trapezoidal plates", *Mater. Des.*, **30**(8), 3030-3035.
- Houmat, A. (2015), "Nonlinear free vibration analysis of variable stiffness symmetric skew laminates", *Euro. J. Mech. A/Solids*, **50**, 70-75.
- Jaberzadeh, E., Azhari, M. and Boroomand, B. (2013), "Thermal buckling of functionally graded skew and trapezoidal plates with different boundary conditions using the element-free Galerkin method", *Euro. J. Mech. A/Solids*, **42**, 18-26.
- Karami, G., Shahpari, S.A. and Malekzadeh, P. (2003), "DQM analysis of skewed and trapezoidal laminated plates", *Compos. Struct.*, **59**(3), 393-402.
- Li, F.M. and Song, Z.G. (2013), "Flutter and thermal buckling control for composite laminated panels in supersonic flow", *J. Sound Vib.*, **332**(22), 5678-5695.
- Malekzadeh, P. (2007), "A differential quadrature nonlinear free vibration analysis of laminated composite skew thin plates", *Thin-Wall. Struct.*, **45**(2), 237-250.
- Malekzadeh, P. (2008), "Differential quadrature large amplitude free vibration analysis of laminated skew plates based on FSDT", *Compos. Struct.*, **83**(2), 189-200.
- Mei, C. and Decha-Umphai, K. (1985), "A finite element method for nonlinear forced vibrations of rectangular plates", *AIAA Journal*, **23**(7), 1104-1110.
- Quintana, M.V. and Nallim, L.G. (2013), "A general Ritz formulation for the free vibration analysis of thick trapezoidal and triangular laminated plates resting on elastic supports", *Int. J. Mech. Sci.*, **69**, 1-9.
- Reddy, J.N. (2004), *Mechanics of Laminated Composite Plates and Shells-Theory and Analysis*, CRC Press.
- Reddy, J.N. and Kuppasamy, T. (1984), "Natural vibrations of laminated anisotropic plates", *J. Sound Vib.*, **94**(1), 63-69.
- Saha, K.N., Misra, D., Ghosal, S. and Pohit, G. (2005), "Nonlinear free vibration analysis of square plates with various boundary conditions", *J. Sound Vib.*, **287**(4-5), 1031-1044.
- Shufrin, I., Rabinovitch, O. and Eisenberger, E. (2010), "A semi-analytical approach for the geometrically nonlinear analysis of trapezoidal plates", *Int. J. Mech. Sci.*, **52**(12), 1588-1596.
- Singha, M.K. and Daripa, R. (2007), "Nonlinear vibration of symmetrically laminated composite skew plates by finite element method", *Int. J. Non-Linear Mech.*, **42**(9), 1144-1152.
- Singha, N.K. and Ganapathi, M. (2004), "Large amplitude free flexural vibrations of laminated composite

- skew plates”, *Int. J. Non-Linear Mech.*, **39**(10), 1709-1720.
- Taj, G. and Chakrabarti, A. (2013), “Static and dynamic analysis of functionally graded skew plates”, *J. Eng. Mech.*, **139**(7), 848-857.
- Tubaldi, E., Alijani, F. and Amabili, M. (2014), “Non-linear vibrations and stability of a periodically supported rectangular plate in axial flow”, *Int. J. Non-Linear Mech.*, **66**, 54-65.
- Wang, X., Wang, Y.L. and Yuan, Z.X. (2014), “Accurate vibration analysis of skew plates by the new version of the differential quadrature method”, *Appl. Math. Model.*, **38**(3), 926-937.
- Yao, G. and Li, F.M. (2013), “Chaotic motion of a composite laminated plate with geometric nonlinearity in subsonic flow”, *Int. J. Non-Linear Mech.*, **50**, 81-90.
- Zamani, M., Fallah, A. and Aghdam, M.M. (2012), “Free vibration analysis of moderately thick trapezoidal symmetrically laminated plates with various combinations of boundary conditions”, *Euro. J. Mech. A/Solids*, **36**, 204-212.
- Zhang, L.W., Lei, Z.X. and Liew, K.M. (2015), “Buckling analysis of FG-CNT reinforced composite thick skew plates using an element-free approach”, *Compos. Part B*, **75**, 36-46.

CC

Appendix

The mass and stiffness matrices in Eq. (8) are assembled from the element mass and stiffness matrices. The element mass and stiffness matrices are written as

$$[M^e] = \begin{bmatrix} M_{uu} & 0 & M_{ubx} \\ 0 & M_{vv} & M_{vby} \\ M_{bxu} & M_{byv} & M_{bxbx} + M_{byby} + M_{bb} \end{bmatrix},$$

where

$$\begin{aligned} [M_{uu}] &= \int_v \rho [H_u]^T [H_u] dv, & [M_{ubx}] &= - \int_v \rho [H_u]^T z \frac{\partial [H_w]}{\partial x} dv, \\ [M_{bxu}] &= - \int_v \rho z \frac{\partial [H_w]}{\partial x} [H_u] dv, & [M_{bxbx}] &= \int_v \rho z^2 \frac{\partial [H_w]}{\partial x} \frac{\partial [H_w]}{\partial x} dv, \\ [M_{vv}] &= \int_v \rho [H_v]^T [H_v] dv, & [M_{vby}] &= - \int_v \rho [H_v]^T z \frac{\partial [H_w]}{\partial y} dv, \\ [M_{byv}] &= - \int_v \rho z \frac{\partial [H_w]}{\partial y} [H_v] dv, & [M_{byby}] &= \int_v \rho z^2 \frac{\partial [H_w]}{\partial y} \frac{\partial [H_w]}{\partial y} dv, \\ [M_{bb}] &= \int_v \rho [H_w]^T [H_w] dv, \\ [K_l^e] &= \begin{bmatrix} K_{00} & K_{0b} \\ K_{b0} & K_{bb} + a_{pbb} \end{bmatrix}, \end{aligned}$$

where

$$\begin{aligned} [K_{00}] &= \int_A [D_0]^T [A] [D_0] dA, & [K_{0b}] &= \int_A [D_0]^T [B] [D_b] dA, \\ [K_{b0}] &= \int_A [D_b]^T [B] [D_0] dA, & [K_{bb}] &= \int_A [D_b]^T [C] [D_b] dA, \end{aligned}$$

in which

$$[D_0] = \begin{bmatrix} \frac{\partial H_u}{\partial x} & 0 \\ 0 & \frac{\partial H_v}{\partial y} \\ \frac{\partial H_u}{\partial y} & \frac{\partial H_v}{\partial x} \end{bmatrix}, \quad [D_b] = \begin{bmatrix} -\frac{\partial^2 H_w}{\partial x^2} \\ -\frac{\partial^2 H_w}{\partial y^2} \\ -2\frac{\partial^2 H_w}{\partial x \partial y} \end{bmatrix}, \quad \{[A], [B], [C]\} = \sum_{k=1}^n \int_{z_{k-1}}^{z_k} [\bar{Q}] \{1 \quad z \quad z^2\} dz,$$

where z_k and z_{k-1} are the coordinates of the upper and lower surfaces of the k th layer in the z direction.

$$\begin{bmatrix} K_{nl}^e \end{bmatrix} = \begin{bmatrix} 0 & K_{0l} \\ K_{l0} & K_{ll} \end{bmatrix},$$

where

$$\begin{aligned} [K_{0l}] &= \frac{1}{2} \int_A [D_0]^T [A] [D_{l1}] [D_{l2}] dA, & [K_{l0}] &= \int_A [D_{l2}]^T [D_{l1}]^T [A] [D_0] dA, \\ [K_{ll}] &= \int_A \left(\frac{1}{2} [D_b]^T [B] [D_{l1}] [D_{l2}] + [D_{l2}]^T [D_{l1}]^T [B] [D_b] + \frac{1}{2} [D_{l2}]^T [D_{l1}]^T [A] [D_{l1}] [D_{l2}] \right) dA, \end{aligned}$$

in which

$$[D_{l1}] = \begin{bmatrix} \frac{\partial H_w}{\partial x} [w_b] & 0 \\ 0 & \frac{\partial H_w}{\partial y} [w_b] \\ \frac{\partial H_w}{\partial y} [w_b] & \frac{\partial H_w}{\partial x} [w_b] \end{bmatrix}, \quad [D_{l2}] = \begin{bmatrix} \frac{\partial H_w}{\partial x} \\ \frac{\partial H_w}{\partial y} \end{bmatrix}.$$